

CYCLE LENGTH DEPENDENCE OF STELLAR MAGNETIC ACTIVITY AND SOLAR CYCLE 23

HWAJIN CHOI^{1,2}, JEONGWOO LEE^{1,3}, SUYEON OH⁴, BOGYEONG KIM¹, HOONKYU KIM¹, AND YU YI¹¹ Department of Astronomy, Space Science and Geology, Chungnam National University, Daejeon, 305-764, Korea² Korea Polar Research Institute, KORDI, Incheon, 406-840, Korea³ Physics Department, New Jersey Institute of Technology, Newark, NJ 07102, USA⁴ Department of Earth Science Education, Chonnam National University, Gwangju, 500-757, Korea

Received 2014 June 24; accepted 2015 January 23; published 2015 March 24

ABSTRACT

Solar cycle (SC) 23 was extraordinarily long with remarkably low magnetic activity. We have investigated whether this is a common behavior of solar-type stars. From the Ca II H and K line intensities of 111 stars observed at Mount Wilson Observatory from 1966 to 1991, we have retrieved data of all 23 G-type stars and recalculated their cycle lengths using the damped least-squares method for the chromospheric activity index S as a function of time. A regression analysis was performed to find relations between the derived cycle length, P_{avg} , and the index for excess chromospheric emission, R'_{HK} . As a noteworthy result, we found a segregation between young and old solar-type stars in the cycle length-activity correlation. We incorporated the relation for the solar-type stars into the previously known rule for stellar chromospheric activity and brightness to estimate the variation of solar brightness from SC 22 to SC 23 as $(0.12 \pm 0.06)\%$, much higher than the actual variation of total solar irradiance (TSI) $\leq 0.02\%$. We have then examined solar spectral irradiance (SSI) to find a good phase correlation with a sunspot number in the wavelength range of 170–260 nm, which is close to the spectral range effective in heating the Earth's atmosphere. Therefore, it appears that SSI rather than TSI is a good indicator of the chromospheric activity, and its cycle length dependent variation would be more relevant to the possible role of the Sun in the cyclic variation of the Earth's atmosphere.

Key words: stars: activity – stars: chromospheres – stars: late-type – stars: magnetic field – Sun: activity

1. INTRODUCTION

The length of the solar cycle (SC) as an important indicator of solar activity was suggested by Friis-Christensen & Lassen (1991) through their study of solar activity and global climate. An impressive agreement found between SC length and northern hemisphere land-surface temperature for the past 130 years shows that the shorter the cycle length, the higher the level of activity of the Sun. Studies to find a stellar counterpart have followed in which a relationship between the chromospheric activity level and cycle length is sought from a large sample of solar-type stars observed over a limited period and is used to reveal possible behaviors of the Sun at a moment of its long-term variability (Soon et al. 1994; Zhang et al. 1994; Baliunas & Soon 1995). The primary data source for the studies on the long-term variation of the chromospheric activity is the systematic Ca II H and K (HK) observation of main-sequence stars that was carried out in the Mount Wilson Observatory (MWO), which operated from 1966 through 1991 (Vaughan et al. 1978; Duncan et al. 1991). Baliunas et al. (1995; hereinafter, B95) presented the data of 111 F2-M2-type stars that turned out to have either particular cycle lengths or invariable. Baliunas & Soon (1995; hereafter, BS95) selected the Sun and 18 solar-type stars, mostly of G0-K7 types and with color indices ($B - V$) in the range of 0.6–1.4, to find a trend that stars during cycles of shorter periods show higher magnetic activity. Such an inverse relationship between the cycle length and brightness variation, if well established for solar-type stars, may provide an insight into the close correlation between the sunspot cycle length and mean terrestrial temperature (Friis-Christensen & Lassen 1991).

In this paper, we investigate whether the low activity level during SC 23 and its unusually long cycle length conform to a statistical relation satisfied by other solar-type stars. Although

the cycle length dependent stellar activity has already been studied as mentioned above, it is of renewed interest because of the unusually long SC 23 and the report of Friis-Christensen & Lassen (1991). The length of SC 23 is estimated to be 13.0 years and that of the preceding SC 22 is as short as 9.2 years (see, e.g., Oh & Kim 2013). A similar pattern is seen for the Dalton Minimum from 1790 to 1830 during which the cycle length had increased from 8.8 to 14.0 years and the Maunder Minimum from 1645 to 1715 was even longer. As in the previous studies, we perform a regression analysis to obtain and elaborate the inverse relationship between the cycle-length and the chromospheric activity level, but with a different data set and analysis method.

In Section 2, we describe the data collection. Section 3 shows our fitting of the data and derivation of activity cycle length. In Section 4, the relation between the variation of chromospheric activity level and stellar cycle length is derived. In Section 5, we compare the regression relation with solar observations. Concluding remarks follow in Section 6.

2. DATA SOURCE AND PREPARATION

Analysis of the observations from the HK Project at MWO have been made in terms of the S index, a ratio of the emission in the line cores to that in two nearby continuum bandpasses on either side of the H and K lines (Vaughan et al. 1978). The S index provides a self-consistent assessment of stellar activity without the need for absolute flux calibration. In this study, we will use the S index as a function of time to derive the cycle length for the sample stars. An issue with the S index is that it depends on color arising from the reference bandpasses and also includes a photospheric contribution in the line core bandpass. For these properties the S index is not an ideal quantity in performing comparisons of stellar activities among

Table 1
Observational Data and Derived Parameters for the G-type Stars

HD Number	Spectral type	Age (Gyr) ^c	$B - V$	$\langle S \rangle$	$\langle R'_{HK} \rangle$	P_{avg} (yr)	P_{B95} (yr)
Sun	G2V	O (4.57)	0.66	0.186	1.392	9.57 ± 0.92	10
1835	G2V	Y	0.66	0.348	3.495	7.26 ± 0.33	9.1
9562	G2V	O	0.64	0.136	0.665	22.62 ± 0.28	Long
10700	G8V	O (5.8)	0.72	0.171	1.102	10.47 ± 0.80	Flat?
20630	G5V	Y (0.3–0.4)	0.68	0.365	3.552	5.41 ± 0.76	5.6
26913	G8V	Y	0.70	0.393	3.853	9.34 ± 4.12	7.8
29645	G3V	O	0.57	0.139	0.731	19.99 ± 5.22	Long
43587	G0V	O	0.61	0.156	0.969	20.81 ± 0.39	Flat?
76151 ^a	G3V	Y	0.67	0.245	2.044	15.22 ± 2.98	2.5
78366	G0V	Y	0.60	0.248	2.438	11.30 ± 2.47	$12.2 + 5.9$
81809	G2V	O	0.64	0.172	1.197	8.34 ± 0.40	8.2
82885*	G8IV-V	Y (1.4–2.3)	0.77	0.286	2.317	10.19 ± 3.53	$7.9 + 12.6$
103095*	G8VI	O (4.7–5.3)	0.75	0.189	1.276	7.52 ± 0.12	7.3
114710	G0V	Y (1.5–2.5)	0.57	0.201	1.741	14.07 ± 1.47	$16.6 + 9.6$
126053 ^a	G3V	O	0.63	0.166	1.129	3.31 ± 1.34	22?
141004	G0V	O (3.8–6.7)	0.60	0.155	0.954	17.53 ± 0.02	Long
143761 ^a	G2V	O (8.7)	0.60	0.150	0.876	9.08 ± 0.09	Long
152391	G7V	Y	0.76	0.392	3.508	10.39 ± 0.54	10.9
161239 ^b	G6V	O	0.65	0.142	0.786	5.65 ± 0.11	$5.7 + 11.8$
176051	G0V	O (2.6–4.3)	0.59	0.176	1.309	10.50 ± 3.25	10?
190406 ^b	G1V	Y	0.61	0.195	1.558	2.62 ± 0.04	$2.6 + 16.9$
206860 ^a	G0V	Y	0.59	0.332	3.733	12.60 ± 0.52	6.2
219834A*	G5IV-V	O	0.80	0.154	0.855	19.41 ± 0.64	21

Note. In the first column, stars marked with * are not main sequence. The superscripts, *a* and *b*, denote discrepancies and outliers excluded from the analysis (see the text for a description). The superscript *c* denotes the ages of stars in the “Age” column were provided by Mamajek & Hillenbrand (2008). “O” (“Y”) stands for old (young) stars. “Flat?” indicates $\langle \sigma_S / S \rangle \approx 1.5\%$, and “Long” means significant variability on timescales longer than 25 years. In spectral-type specifiers, IV, V, and VI denote subgiant, main sequence plus dwarf, and subdwarf, respectively.

different spectral-type stars. Another dimensionless index called R'_{HK} can be used to represent stellar chromospheric activity, which is the chromospheric flux in Ca II *H* and *K* passbands divided by the total bolometric flux with the photospheric contribution removed (Middelkoop 1982; Noyes et al. 1984). We will use R'_{HK} index in comparing the level of chromospheric activity of stars with each other.

We must note that the original raw data of the HK project are no longer accessible. We thus had to retrieve the S and R'_{HK} indices by digitizing the data from old published figures. We were able to collect data of all 23 G-type stars out of the 111 stars in the B95’s data set. We used, for the digitization, software called *Engauge*.⁵ The uncertainty associated with the digitization itself is small; our digitized S index and those of B95, show relative differences by less than 1%. In addition, the S indices read out as monthly mean were converted to yearly mean to further reduce the uncertainty. In Table 1, we list the HD numbers, spectral types, $B - V$ color indices, and ages of the 23 G-type stars. Spectral type and $B - V$ are taken from B95, and age is expressed either in units of Gyr (from Mamajek & Hillenbrand 2008) or simply as O (old) or Y (young) based on the previous studies (Vaughan 1980; Noyes et al. 1984). The next three columns list the yearly mean of S and R'_{HK} indices and the cycle length P_{avg} that we calculated from the aforementioned data. The last column lists the cycle length determined by B95 for comparison with ours. As seen in the table, our data set contains a stellar spectral-type ranging from G0 to G8 mostly belonging to the main sequence with exceptions denoted by asterisks (HD 82885, HD 103095, HD 219834A) and the color index ($B - V$) ranging from 0.57 to

0.80. As we only intend to limit the data set to G-type stars only, the number of stars may seem to be relatively small. However, it still is the largest dataset for G-type stars available at present.

3. CYCLE LENGTH DETERMINATION

Activity cycle length is determined from the S index plotted as a function of time. B95 determined the activity cycle period using Periodogram (Scargle 1982). In this study, we use a routine called MPFIT (Markwardt 2009) implemented in the Interactive Data Language to perform a curve-fitting of the data to sine functions. The MPFIT solves nonlinear least squares problems using the Levenberg-Marquardt Technique, also known as the damped least-squares method (Levenberg 1944). In our analysis, the model is a combination of two sine functions as shown in Equation (1) and fitting of data to this model is made by varying the relative amplitudes, $a_{1,2}$, of the two sine functions as well as period ($P_{1,2}$) and phases ($\phi_{1,2}$):

$$S = a_1 \sin \left(2\pi \frac{t}{P_1} + \phi_1 \right) + a_2 \sin \left(2\pi \frac{t}{P_2} + \phi_2 \right) + C \quad (1)$$

where time t is in years, and C is a constant. Between the two periods, $P_{1,2}$, we take the period of the one associated with larger amplitude as the representative length of the cycle. In the fitting, we exclude the portions that are not considered to be of the sine function, for example, those with either a linear portion or seemingly of secondary oscillation. Consequently, this approach ensures determination of a single period. While this

⁵ <http://digitizer.sourceforge.net/>

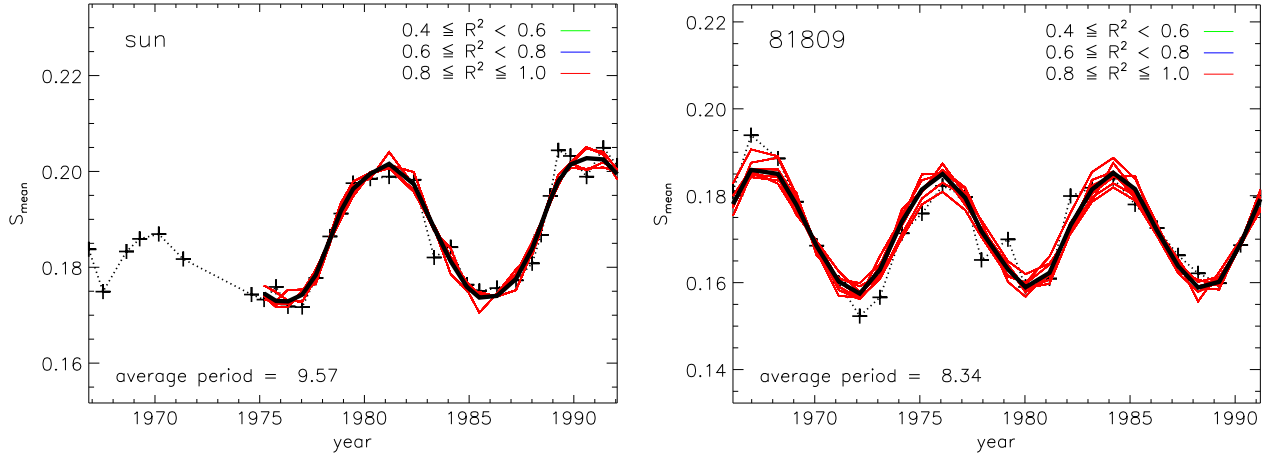


Figure 1. Annual mean S index with sine curve fitting for the Sun and HD 81809. Both belong to a group of stars with relatively large amplitudes within one cycle. The curves are colored to show the goodness of fit. The green colored curves have $0.4 \leq R^2 < 0.6$, blue for $0.6 \leq R^2 < 0.8$, and red for $0.8 \leq R^2 \leq 1.0$. The bold black line is the averaged regression curve so that it has $0.4 \leq R^2 \leq 1.0$. Averaged period, P_{avg} , is computed by fitting sine curves to the black line.

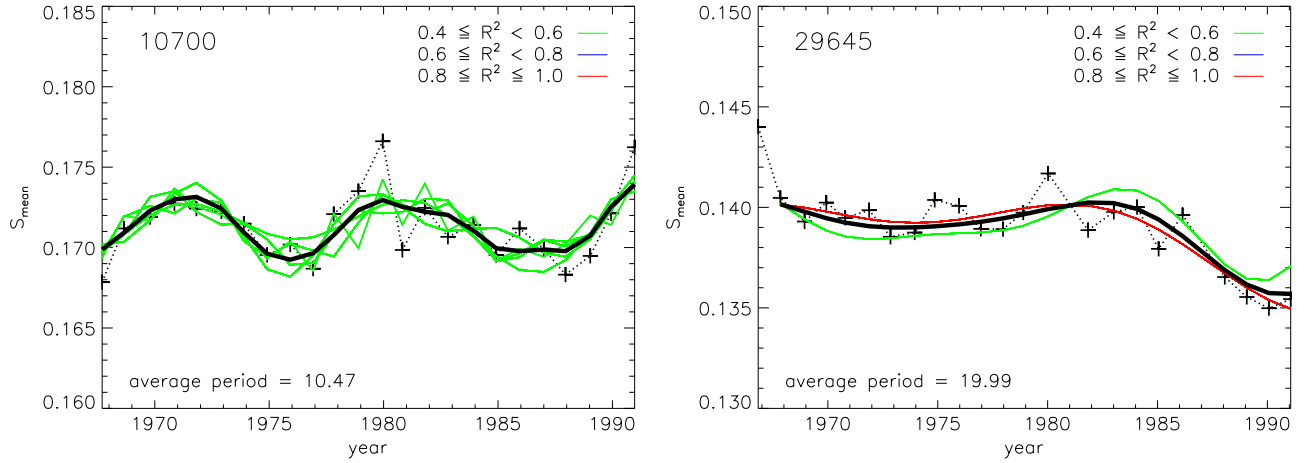


Figure 2. Annual mean S index with sine curve fitting for HD 10700 and HD 29645, which have relatively long periods and small amplitudes within each cycle. The same color scheme as in Figure 2 is used.

treatment may be subjective, the idea is that cycle length should be determined from the period of standard activity variation. For instance, we would exclude the portion of the Maunder Minimum when determining the typical length of SC. The goodness of the fit is measured by the coefficient of determination, R^2 , the ratio of the residual sum of squares to total sum of squares. In general, $R^2 > 0.6$ is considered to be a strong correlation. In the present fitting, we only consider the set of sine functions that give $R^2 > 0.4$.

Figure 1 shows the annual mean S parameter as a function of time along with the fitting functions for the Sun (left panel) and HD 81809 (right panel), which are among the relatively strong magnetic activity, i.e., large amplitudes of the S variation within each cycle. The cross-patched dotted lines represent actual data. The regression curves are color coded according to R^2 : green for $0.4 \leq R^2 \leq 0.6$, blue for $0.6 \leq R^2 \leq 0.8$, and red for $0.8 \leq R^2 \leq 1.0$. The thick black line is the average of all fittings for ($0.4 \leq R^2 \leq 1.0$). We finally determine the average period, P_{avg} , from the black curve. P_{avg} is denoted in the lower left corner of each panel. On the other hand, Figure 2 shows samples of weaker magnetic activity, HD 10700 (left panel) and HD 29645 (right panel). The fitting results for these stars are shown with the same color convention as in Figure 2. Obviously, the fit is relatively poor for the stars with small

amplitudes and long periods, and it is more difficult to determine the cycle length of such stars. Nonetheless, we were able to determine the cycle lengths for all 23 stars, while some of them remained undetermined in B95 as listed in Table 1.

As listed in the last two columns of Table 1, the cycle lengths P_{avg} derived in the present study and those originally presented in B95 agree fairly well with each other as expected. However, there are some discrepancies, as we present specific values for a few stars that were assigned by B95 to either “Long,” “Flat,” or some numbers with question marks. B95 considered that the cycle lengths for those stars were either longer than 25 years or undeterminable, whereas our method practically forces the determination of single cycle length assuming that solar-like stars have single dominant cycle length. In this case, we have two options. If we also find a cycle length to be long but finite (say, ≥ 17 yr) we regard our result as more reliable to include it in further analysis. If our cycle length is short (< 17 years) for a star classified as “Long” (e.g., HD 143761), we consider both results controversial, and exclude them from further analysis. In this way, those stars for which our P_{avg} differ from P_{B95} by more than 30% are marked with superscript, a . In addition, HD 190406 and HD 161239 are marked b , because they have cycle lengths shorter than six years, far below typical SC length, and are not very relevant for

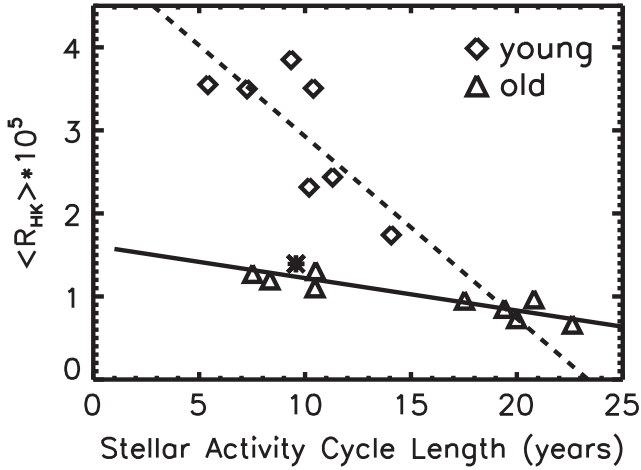


Figure 3. Relationship between P_{avg} and $\langle R'_{HK} \rangle$ under the linear regression. The diamond (triangle) symbols represent young (old) stars and the asterisk symbol represents the Sun. The lines are the regression curves.

Table 2
Regression Parameters and the Coefficients of Determination

Group	$a[10^{-5}]$	$b[10^{-5}]$	R^2
All	3.5	-0.14	0.42
Young	5.1	-0.22	0.58
Old	1.6	-0.039	0.83

our purpose. Thus the total six stars marked with either a (discrepancies) or b (outlier) are excluded from further analysis.

4. CYCLE LENGTH AND BRIGHTNESS VARIATION

As mentioned in Section 2, the S index may be inadequate for performing comparisons of stellar activities among different spectral-type stars, and another index R'_{HK} is preferred to represent the actual level of stellar chromospheric activity (Middelkoop 1982; Noyes et al. 1984). R'_{HK} is defined as the chromosphere flux F'_{HK} in Ca II H and K passbands divided by the total bolometric flux, $F_{\text{bol}} = \sigma T_{\text{eff}}^4$, and R'_{HK} so that

$$R'_{HK} = \frac{F'_{HK}}{\sigma T_{\text{eff}}^4} = R_{HK} - R_{\text{ph}}. \quad (2)$$

In the RHS, R_{HK} is related to the S index if the color-dependent conversion factor C_{cf} is known: $R_{HK} = F_{HK}/\sigma T_{\text{eff}}^4 = 1.340 \times 10^{-4} C_{cf} S$ (Noyes et al. 1984). In this way, R'_{HK} can be computed from the S index and is an adequate quantity for use in comparison of chromospheric activity among different spectral types, because it is the fraction of a star's bolometric luminosity radiated as chromospheric H and K emission with the photospheric contribution removed.

In Figure 3, we plot R'_{HK} against the average cycle length, P_{avg} , for 17 stars with symbols. The single asterisk symbol represents the Sun ($\langle R'_{HK} \rangle = 1.392$) and lines are regression curves in the form: $R'_{HK} = a + bP_{\text{avg}}$. It is apparent from Figure 3 that a stronger relation may result if the regression analysis is made for two separate groups as denoted by different symbols in the figure. We thus divide all stars into two groups depending on whether they are more active ($R'_{HK} \geq 1.5 \times 10^{-5}$) or less active ($R'_{HK} < 1.5 \times 10^{-5}$). The

derived values of a , b , and the goodness of the fit R^2 (coefficient of determination) are listed in Table 2, and the regression lines are plotted in Figure 3 as dashed and solid lines. The distinction between these two groups is associated with the age of stars. Table 1 lists ages of nine stars taken from Mamajek & Hillenbrand (2008). The average age of stars in the first group is 1.4 ± 0.91 Gyr and that in the second group is 4.81 ± 0.88 Gyr. For the young stars, the activity level, R'_{HK} , changes more rapidly with cycle length, P_{avg} , but for the old stars, R'_{HK} varies very slowly with P_{avg} .

Finally, we insert the $R'_{HK}-P_{\text{avg}}$ relation (with parameters from Table 2) into the empirical relation between the brightness variation, ΔB , and that of R'_{HK} index established for the Sun and solar-type stars $\Delta B [\%] = (8.0 \pm 4.0) \times 10^4 \Delta R'_{HK}$ (Zhang et al. 1994). This allows us to calculate the relative variation of brightness ΔB as a function of cycle length change, ΔP_{avg} . Our best prediction for the cycle length dependent variation of stellar brightness is obtained under the linear regression of solar-type stars (G-type stars with $R'_{HK} < 1.5 \times 10^{-5}$). For those stars, we find a simple expression for ΔB and ΔP_{avg} in the form

$$\Delta B [\%] = 0.031(1 \pm 0.5) \Delta P_{\text{avg}} [\text{yr}]. \quad (3)$$

Note that the relatively large uncertainty range (50%) in this relation is introduced from the $\Delta B-\Delta R'_{HK}$ relation (see the discussion below).

The above equation is the main result of the present study. We must note that the above result is not very different from the earlier result of BS95, by which we refer to that fact that differentiation of Equation (1) of BS95 and substitution of Equation (2) from Zhang et al. (1994) gives a similar relation for ΔB and ΔP_{avg} as above. The similarity deserves several remarks. (1) These two results were obtained from different data sets. In the present study, we have utilized a more selective sample of 23 G-type stars whereas BS95 used the Sun and 18 solar-type stars including both G and K dwarfs, and supplemented the stellar data with as many solar data from the record as presented in their Figure 3. We thus expect that both data sets yield regression results weighted toward solar-type stars. (2) We have calculated the cycle lengths using a different method and also used digitized data (see Section 2). It is, however, unlikely that these would introduce many differences. A more significant difference lies in our approach of determining only single periods under the assumption that the cycle length should be searched for in the period of cyclic variation based on the Sun's behavior. This allowed us to include a few more stars that had not been classified as either *Long* or *Flat* in BS95. (3) The most obvious difference of the present work from BS95 is the finding of a segregation between *young* and *old* solar-type stars in the empirical relationship between the chromospheric activity and activity cycle length. We thus presented two distinct linear regressions best representing the two groups and the result for the old star group agrees to the earlier finding of BS95. In summary, we used a data set more restricted in terms of spectral range and stellar age along with a more aggressive search for the cycle lengths. The reason why we nonetheless found a regression relation similar to that of BS95 is probably that both data sets well represent the solar-type, solar-age stars.

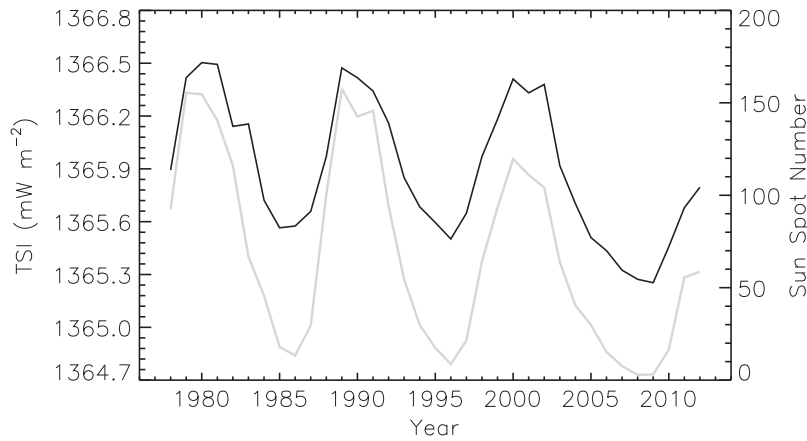


Figure 4. Variation of TSI over the recent three solar cycles. The black (gray) solid line represents the yearly averaged TSI (SSN).

5. SOLAR IRRADIANCE VARIATIONS

We now compare the above prediction of brightness variation with cycle length with actual solar measurements, either total solar irradiance (TSI) or spectral solar irradiance (SSI). Figure 4 shows TSI together with sunspot number (SSN) as black and gray solid lines, respectively. The TSI data are obtained from Physikalisch-Meteorologisches Observatorium Davos World Radiation Center, and the data of SSN from the National Geophysical Data Center, respectively. The TSI variation is well in phase with SC (as represented by SSN), but the amount of variation is very small. From maximum to minimum within a cycle, TSI changes only $\sim 0.1\%$. The inter-cycle variation of TSI is more obvious in the minimum than maximum. TSI changed from SC 22 to 23 by -0.0046% from the maximum of Cycle 22 to the maximum of Cycle 23 and -0.018% from the SC 22 minimum to the SC 23 minimum. Now the regression relation (Equation (3)) indicates that solar brightness should have changed from SC 22 ($P_{\text{avg}} = 9.2$ yr) to SC 23 (13.0 yr) by $(-0.12 \pm 0.06)\%$. This is much higher than the observed -0.018% from the SC 21 minimum to the SC 22 minimum even though account for the relatively large uncertainty range and only the minimum-minimum difference.

We then check SSI for a possibility that the missing component is confined to a specific wavelength range. SSI data are obtained from the LASP Interactive Solar Irradiance Datacenter, which is composite UV irradiance data⁶ constructed from six independently measured data sets for the time period from 1978 to 2005 (DeLand & Cebula 2008). Figure 5 shows the SSI at four selected wavelength intervals as functions of time. Both daily and yearly averaged SSI data are shown together with SSN (blue curves) as reference. While the original data covers the wavelength range 120–400 nm in 1 nm bins and plotted here are running averages over a timescale of one year and a 5 nm wavelength interval. Apparently, SSI exhibits a larger variation than TSI; the maximum to minimum variation within cycle SSI variability varies by 3%–9% (Table 2 of DeLand & Cebula 2012). The time variation pattern of SSI is not uniform across at wavelengths, and this is one reason why inter-cycle variation of TSI is so small. In some wavelengths, SSI does not show a cyclic variation pattern at all, while it does at some other wavelengths. In this figure, only the SSI at 200–205 nm shows

a high correlation with SSN. Since the goal of the present study is to find the SC-dependent variation of irradiance, we change the focus to a search for the spectral range where the SSI's behavior matches that of SC well. Figure 6 shows the coefficient of correlation between the time profile of SSI and that of SSN as a function of wavelength. We note that SSIs are averaged over a time interval of a year and over each wavelength interval of 5 nm before the correlation analysis. If we set the coefficient above 0.6 as the criterion for the good correlation, our result indicates that the cyclic behavior is well seen the waveband from 170 nm to 260 nm. This spectral region does not exactly overlap but is close to the 200–250 nm range that has been quoted in previous works as the spectral range where the solar UV radiation can be absorbed in the thermosphere and ionosphere to drive atmospheric heating.

6. CONCLUDING REMARKS

In an attempt to better understand the unusual behaviors of the recent SCs, we have re-examined the relation between the excess chromospheric activity and the cycle length change using a more selective sample of stars, namely, all G-type stars in the Mt. Wilson data set with color index ($B - V$) in the range 0.6–0.8. The ages are also constrained to 5.0–5.5 Gyr corresponding to the low activity $R'_{\text{HK}} \leq 1.5 \times 10^{-5}$. As a result, we found a strong correlation between R'_{HK} and P_{avg} with 83% confidence. The relation itself is not very different from the earlier result by BS95. We once again emphasize that these two results were obtained from different sets of data, and thus assuring its reliability. The principal contribution of the present work to this type of study is, however, the finding of a segregation of young and old solar-type stars in the empirical relationship between the chromospheric activity index and activity cycle length, and the strong correlation between R'_{HK} and P_{avg} is found for the old solar-type stars.

An issue arises in the next step of building a relation between the brightness variation with cycle length change. Using Zhang et al.'s (1994) $\Delta B - \Delta R'_{\text{HK}}$ relation, our regression model predicts the relative change of solar brightness by $(0.12 \pm 0.06)\%$ during the transition from the SC 22 minimum to SC 23 minimum, which turns out to be much higher than the actually measured TSI variation $\leq 0.018\%$. As a comparison, we note that BS95 used their regression relation to infer a 0.4% change in TSI around the Maunder Minimum, which was also found too high by subsequent works (e.g., Wang et al. 2005).

⁶ <http://lasp.colorado.edu/lisird/cssi/>

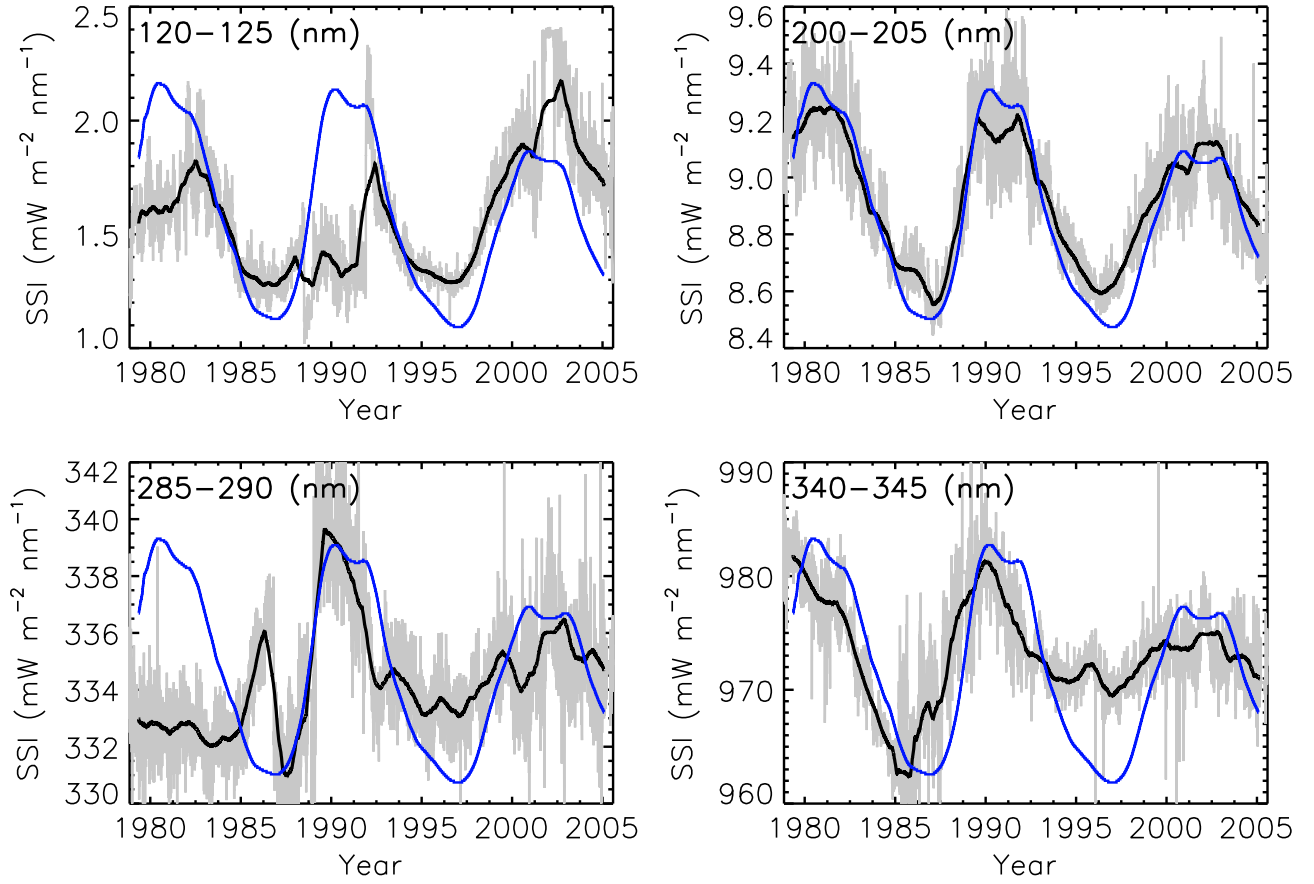


Figure 5. Variation of SSI over the recent three solar cycles. The black (gray) solid lines represent the yearly (daily) average SSIs at four selected wavebands as denoted in the upper left corner of each panel. The blue lines in all panels are the yearly average SSN.

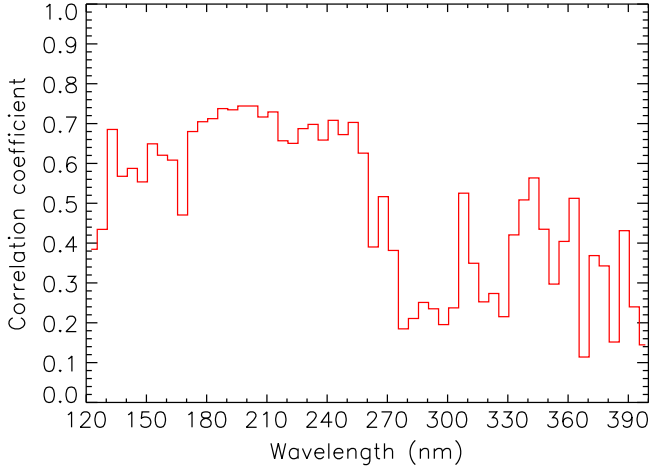


Figure 6. Correlation coefficient of SSI and SSN as a function of wavelength.

For this discrepancy, we may consider two possibilities: (1) the Sun is an unusual star undergoing a much less brightness variation in response to the change of cycle length than other stars, and (2) the Sun is a typical star and the relation between $\Delta R'_{HK}$ and ΔB should be reconsidered. To answer this question, we need to know about the cycle-length dependence of the flux in the visible band (400–900 nm) as well, because it contributes to the total solar luminosity by almost 50%. The

present study, however, found that the Sun behaves like a typical average star as far as the R'_{HK} – P_{avg} relation is concerned. It is therefore likely that the visible band flux is decorrelated with the UV flux represented by R'_{HK} . This means that R'_{HK} is not a good indicator of TSI unlike the early result by Zhang et al. (1994, their Equation (2)) that is based on only 10 stars and also may include stars that subsequently have been proven not to be solar-like, but are evolved stars (Wright 2004).

We briefly discuss why R'_{HK} may not be a good indicator of TSI. Ca II core emission strength reflects the area coverage of faculae on the solar disk where UV emission is also strong. Ca II emission is therefore strongly correlated with the far-UV flux. On the other hand, sunspots are the most obvious source of solar variability in the visible band, but spot filling factor and facular disk coverage are not necessarily correlated to each other. It then follows that the Ca II K-line flux may not be correlated with variability in the visible band. In this case, R'_{HK} is an unreliable indicator for the brightness change in the visible band and thus not for TSI as well. This conclusion is corroborated to some extent by Figure 6, which suggests an overall declining trend in correlation coefficient of SSI with SSN toward longer wavelengths.

However, R'_{HK} is a good indicator of SSI in the far-UV. In this regard, we believe it an important result that the temporal variation of SSI shows a high correlation with SSN in the wavelength range, 170–260 nm, close to the spectral range where the solar UV radiation can be absorbed into the

thermosphere and ionosphere. For this reason, the cycle-length dependent variation of SSI should be regarded more important to the heating of the Earth's atmosphere than that of TSI. To quantitatively support the proposal of Friis-Christensen & Lassen (1991) we, however, need a more detailed mechanism for converting the SSI to heating of the Earth's atmosphere, which is unavailable at present. We only suggest the possibility of SSI as a driver for terrestrial climate only on a qualitative basis. Future studies should pursue this question with physics-based models for solar UV radiation and coronal magnetic activity together with proxy indicators such as solar magnetograms and the Mg II index (Heath & Schlesinger 1986).

We thank the referee for a number of important comments that greatly helped us to prepare this paper in the present form. This research was supported by national nuclear R&D program through the National Research Foundation of Korea (NRF) grant funded by the Korean government (MSIP; 2014M2B2A9032253) and by Space Core Technology Development Program through the Ministry of Education, Science and Technology (MEST; 2012M1A3A3A02033496). J. L. was supported by the Brainpool program 2014 of KOFST.

REFERENCES

- Baliunas, S. L., Donahue, R. A., Soon, W. H., et al. 1995, *ApJ*, **438**, 269
 Baliunas, S. L., & Soon, W. H. 1995, *ApJ*, **450**, 896
 DeLand, M. T., & Cebula, R. P. 2008, *JGR*, **113**, A11103
 DeLand, M. T., & Cebula, R. P. 2012, *JASTP*, **77**, 225
 Duncan, D. K., Vaughan, A. H., Wilson, O. C., et al. 1991, *ApJS*, **76**, 383
 Friis-Christensen, E., & Lassen, K. 1991, *Sci*, **254**, 698
 Heath, D. F., & Schlesinger, B. M. 1986, *JGR*, **91**, 8672
 Kuhn, J. R., & Libbrecht, K. G. 1991, *ApJ*, **381**, 35
 Levenberg, K. 1944, *QApMa*, **2**, 164
 Mamajek, E. E., & Hillenbrand, L. A. 2008, *ApJ*, **687**, 1264
 Markwardt, C. B. 2009, in *ASP Conf. Series*, Vol. 411, *Astronomical Data Analysis Software and Systems XVIII*, ed. D. A. Bohlender, D. Durand, & P. Dowler (San Francisco, CA: ASP), 251
 Mauquoy, D., Geel, B., Blaauw, M., & Plicht, J. 2002, *The Holocene*, **12**, 1
 Middelkoop, F. 1982, *A&A*, **107**, 31
 Noyes, R. W., Hartmann, L. W., Baliunas, S. L., Duncan, D. K., & Vaughan, A. H. 1984, *ApJ*, **279**, 763
 Oh, S., & Kim, B. 2013, *JASS*, **30**, 101
 Scargle, J. D. 1982, *ApJ*, **263**, 835
 Soon, W. H., Baliunas, S. L., & Zhang, Q. 1994, *SoPh*, **154**, 385
 Vaughan, A. H., Preston, G. W., & Wilson, O. C. 1978, *PASP*, **90**, 267
 Vaughan, A. H. 1980, *PASP*, **92**, 392
 Viereck, R. A., Floyd, L. E., Crane, P. C., et al. 2004, *SpWea*, **2**, S10005
 Wang, Y.-M., Lean, J. L., & Sheeley, N. R. 2005, *ApJ*, **625**, 522
 Willson, R. C., & Hudson, H. S. 1991, *Natur*, **351**, 42
 Wright, J. T. 2004, *AJ*, **128**, 1273
 Zhang, Q., Soon, W. H., Baliunas, S. L., et al. 1994, *ApJL*, **427**, L111